INSTITUTE OF PHYSICS PUBLISHING MODELLING AND SIMULATION IN MATERIALS SCIENCE AND ENGINEERING

Modelling Simul. Mater. Sci. Eng. **14** (2006) 721–731 doi:10.1088/0965-0393/14/4/013

Embedded atom method potentials employing a faithful density representation

P Mitev[1], **G A Evangelakis**[1] **and Efthimios Kaxiras**[2,3]

[1] Department of Physics, University of Ioannina, Ioannina, Greece 45110
[2] Department of Materials Science and Technology, University of Ioannina, Ioannina, Greece 45110

Received 28 September 2005, in final form 29 March 2006
Published 15 May 2006
Online at stacks.iop.org/MSMSE/14/721

Abstract

We present an approach for deriving embedded atom method energy functionals which employs a faithful representation of the valence electron that reproduces *ab initio* electronic structure calculations. This approach offers the possibility of improved accuracy and versatility over existing methods. Moreover, the approach has a distinct advantage for coupling to more accurate methods in the context of multiscale schemes. The embedding function is based on first breaking down the electronic density to individual atomic contributions and then designing an interatomic function which captures the interaction between the atomic contributions towards formation of the interatomic bonds. We use Al as a prototypical metallic solid to illustrate the application of the method and we employ density functional theory (DFT) to calculate the electronic charge densities and energies for determining the values of fitting parameters. We validate the approach by reproducing adequately experimental data for the cohesive energy, bulk modulus, elastic constants and dynamical properties at finite temperatures, obtained by molecular dynamics simulations.

1. Introduction

The embedded atom method (EAM) has become a popular method for computing many static and dynamical properteis of metallic systems, in particular, for situations where a large number of atoms are required to capture the physics. The conceptual basis of the method rests on the notion that the energetics of an atom placed in the environment of a solid depends on the electron density of the host atoms alone, an idea first put forward by Norskov and Lang [1] and by Scott and Zaremba [2]. Following this abstract formulation, Norskov [3] and Daw and Baskes [4]

[3] Work performed while on leave from Department of Physics and Division of Engineering and Applied Sciences, Harvard University, Cambridge MA 02138, USA.

produced practical schemes for implementing the idea in calculations of the properties of metallic systems. Voter [5] has provided a comprehensive and insightful review of the standard EAM approach for metallic systems. A wealth of molecular dynamics (MD) and Monte Carlo (MC) simulations established this approach as a very successful compromise between computational efficiency and accuracy of describing metals and alloys without recourse to quantum mechancical approaches that can provide higher accuracy but at a much greater computational cost (see, for example, [6,7]). The original method was subsequently expanded by Baskes [8] to treat solids with highly directional distributions of valence electron densities, that is, covalent bonding, thus allowing for a much wider scope of applications.

The method is empirical, as it relies on the use of data (either from experiment or from higher level theory) for fitting the necessary parameters for the description of a particular material. However, several deficiencies have appeared in many of the applications of the original formulation. A case in point is the properties of an impurity which, in terms of the usual EAM approach, are supposed to be fully characterized by the classical pair potential term and the embedding potential term, which together comprise the energy functional, while the local density of the embedded atom at the impurity site remains unaffected by the presence of the impurity. In this sense, the embedding function is designed for the description of the embedded atom only, while the total charge density is characteristic of the local environment, which is a reasonable approximation in the case of bulk stoichiometric materials but is an oversimplification in the cases of impurities or point defects, where the local electronic density has contributions from the host and and the embedded atom. The problem is equally important when dealing with binary or ternary alloys, while non-stoichiometric or multi-element materials remain an impervious challenge.

The aim of the present work is to construct a potential model within the framework of the EAM theory, able to capture the interactions between atoms in specific local environments. In traditional EAM approaches, the parameters that enter into the various terms of the total energy are fixed by reproducing experimental values for certain key properties of the solid, such as the cohesive energy, the equilibrium volume per atom, bulk and elastic moduli, etc. Within this formulation, all quantities that appear in the energy functional, including the electronic density, are treated as fitting parameters whose values are adjusted to produce the best results without imposing restrictions from physical considerations. The success of the method in its traditional incarnations is attributed to the ability of the embedding functional $F(\overline{\rho}_i)$, where $\overline{\rho}_i$ is the effective density at the position of the embedded atom labelled i, to capture the many-body effects of placing an atom in the environment of the solid. A key difference in the present work compared with the previous approaches is that the electronic density is not viewed as a fitting parameter but as a quantity that accurately reproduces the 'true' valence densities, obtained from *ab initio* calculations, in the regions of interest. Such an approach had been considered before by Foiles *et al* [9], but the authors focused on reproducing the atomic densities of isolated atoms. In contrast, the present work focuses on reproducing the *ab initio* density of the ground-state solid phase. To justify our approach, we appeal to common knowledge that the embedding functional is intimately connected to the notion of bond-order, which had been deliberately built into the EAM formalism by its creators. Careful studies by Robertson and co-workers [10–12] have examined the bond-order aspect of EAM by comparing *ab initio* and EAM-type calculations for a wide range of Al structures. This notion is succinctly captured in Voter's review article by the following quote: 'The many-body effect of $F(\overline{\rho}_i)$ is that, as an atom makes more bonds, each new bond is weaker than the previous one; making a new bond increases the total bonding energy, but decreases the average energy per bond.' [5] In this sense, our approach in formulating and parametrizing $F(\overline{\rho}_i)$ puts a premium on an exact representation of the density in the

regions *between* atoms, where electron sharing, that is, formation of chemical bonds takes places.

In the following, we first describe the method in section 2, provide an application for Al, a prototypical metallic solid, in section 3 and finally conclude with remarks about the prospects of the method in section 4.

2. The method: construction of new EAM potentials

The fundamentals of the method have been discussed in the literature in detail (see for example review [5]), so only some important aspects necessary for the discussion of the present work will be given here. In the embedded atom approach for a one-component system, the potential energy contribution to the total energy of an atom labeled i is written as

$$E_i = F(\overline{\rho}_i) + \frac{1}{2}\sum_{j\neq i}\phi(R_{ij}), \tag{1}$$

where R_{ij} is the distance between atoms i and j, $F(\overline{\rho}_i)$ is the 'embedding energy' as a function of the host density at the position of atom i, $\overline{\rho}_i$, due to all its neighbours j, given by

$$\overline{\rho}_i = \sum_{j\neq i}\rho^{\mathrm{eff}}(R_{ij}) \tag{2}$$

with both $\rho^{eff}(R_{ij})$ and $\phi(R_{ij})$ effective pairwise interactions. The first term in equation (1) is volume dependent and represents, in an approximate manner, the many-body interactions of the system. While the functional of equation (1) is based on certain physical ideas regarding the bonding in metallic systems, in actual implementations the functions $\rho^{eff}(R)$, $F(\overline{\rho})$, $\phi(R)$ have lost their ties with the original physical meaning and are treated as purely fitting quantities that are parametrized in some reasonable way, the only requirement being that the resulting functional reproduces well the target data from the experiment or higher level theory (the 'electron density', for instance, is even allowed to take negative values).

Our approach consists of the following two steps.

(i) We first construct a charge density, consisting of superposition of atomic-like charge densities, which faithfully reproduces the density obtained from *ab initio* calculations.

(ii) Using the atomic-like charge densities, we construct an effective charge density which only depends on the distance between pairs of atoms and is chosen to emphasize the formation of interatomic bonds; this effective charge density is employed in an embedding functional similar to $F(\overline{\rho}_i)$ in equation (1).

We describe next these two steps in detail.

2.1. Faithful representation of charge density

The starting point is the decomposition of the total electron density obtained from *ab initio* calculations. Here and in the rest of the paper, *ab initio* results refer to calculations using density functional theory (DFT) [13], including the valence electrons only through the use of pseudopotentials, and the local-density approximation [14] for the exchange-correlation energy of the electron gas, as parametrized by Perdew and Zunger [15]. All the DFT calculations were performed with the HARES code [16, 17].

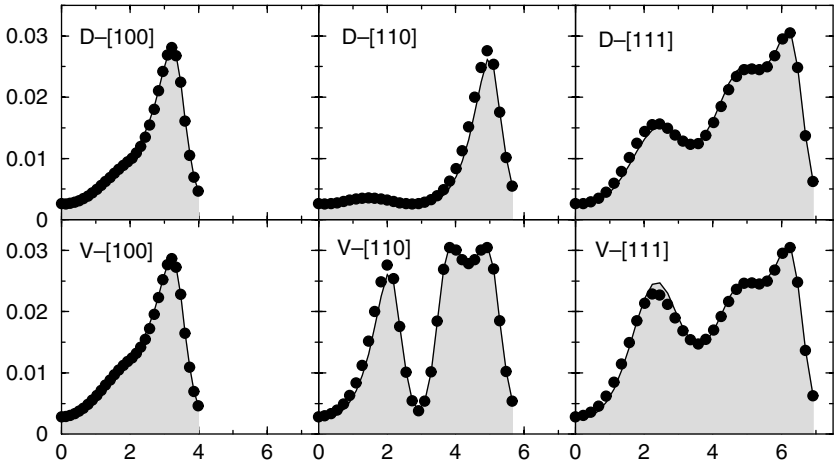

Figure 1. Representative charge densities (in a.u.$^{-3}$) at cross sections along selected directions for the vacancy (denoted V, bottom row) and the divacancy (denoted D, top row) in bulk Al. The lines are first-principles results; the symbols are fitted values. The directions of the cross sections are given in each panel. The horizontal axes are in Å.

We construct first a basis for expressing the individual atomic contributions $q_i(\boldsymbol{r})$ to the total density $\rho_{\rm tot}$ $(\boldsymbol{r})$ by adopting the expression:

$$\rho_{\rm tot}(\boldsymbol{r}) = \left[\sum_{l=0,1} t^{(l)} \left(q^{(l)}(\boldsymbol{r})\right)^2\right]^{1/2} \tag{3}$$

$$q^{(0)}(\boldsymbol{r}) = \sum_i \rho^{(0)}(r_i) \tag{4}$$

$$q^{(1)}(\boldsymbol{r}) = \left[\sum_{\alpha=x,y,z} \left(\sum_i \frac{\alpha_i}{r_i}\rho^{(1)}(r_i)\right)^2\right]^{1/2} \tag{5}$$

with $\boldsymbol{r}_i = \boldsymbol{r} - \boldsymbol{R}_i$ and $r_i = |\boldsymbol{r}_i|$, where $\boldsymbol{R}_i$ is the position of ion i, containing s-type (superscript 0) and p-type (superscript 1) of angular momentum contributions. The summations over ion positions i extend over all ions within a distance $R_c = 6.01$ Å from the point $\boldsymbol{r}$ where the density $\rho_{\rm tot}(\boldsymbol{r})$ is being evaluated. For the individual anglular momentum components of the density we adopt the expression

$$\rho^{(l)}(r) = \left(a_0^{(l)} + a_1^{(l)} r + a_2^{(l)} r^2\right)^2 \exp(-r/c^{(l)}), \qquad l = 0, 1. \tag{6}$$

The choice of this representation for $\rho^{(l)}(r)$ corresponds to the $3s$ wavefunction, a case relevant to the application for Al presented in section 3. The parameters that appear in the above expressions, namely $t^{(l)}, a_k^{(l)} (k = 0, 1, 2), c^{(l)}$ with $l = 0, 1$, can now be fitted to reproduce the desired charge density in the solid $\rho_{\rm tot}(\boldsymbol{r})$.

As an example, we performed such a fit to reproduce the charge density of bulk Al at its equilibrium lattice constant; the parameters for this fit are given in table 1. The fit to determine the values of the parameters, as well as all subsequent fits in the present work, were performed using the MERLIN minimization package [18]. This fit is excellent, yielding a maximum deviation from *ab initio* results of less than 2% near the ionic positions, with even better agreement (less than 1% difference) in the interatomic regions which are of greater physical interest.

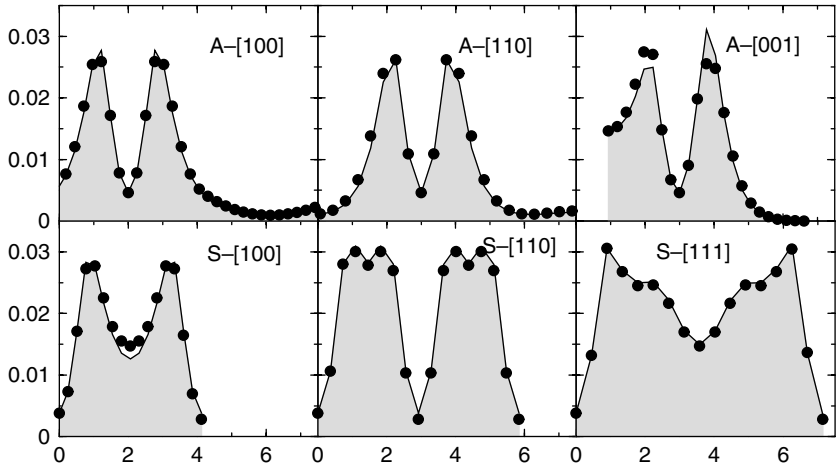

Figure 2. Representative charge densities (in a.u.$^{-3}$) at cross sections along selected directions for the (100) surface of Al (denoted S, bottom row) and one adatom on that surface (denoted A, top row). The lines are first-principles results; the symbols are fitted values. The directions of the cross sections are given in each panel. The horizontal axes are in Å.

Table 1. Values of the parameters that appear in equations (3)–(6) for Al.

	Value	
Parameter	$l = 0$	$l = 1$
$t^{(l)}$	1.0000	0.9486
$a_0^{(l)}$	−2.1927	−3.5598
$a_1^{(l)}$	1.9925	1.3753
$a_2^{(l)}$	−0.3074	−0.2624
$c^{(l)}$	0.2154	0.1838

Moreover, the fit is also remarkably transferable: even though it was derived from bulk results, it reproduces the charge density near bulk defects, ideal surfaces and other surface features. To demonstrate this success, we compared the charge density computed from *ab initio* results and that obtained from the present approach in the neighbourhood of a vacancy and a divacancy in bulk Al (figure 1), as well as on the flat (100) surface and in the neighbourhood of an adatom on that surface (figure 2). The agreement with the *ab initio* results is excellent, with the only discernible small differences found in the case of the adatom along the [100] and [001] directions.

2.2. Embedding functional

Next we need to construct a quantity that relies on the individual charge densities and can be used to obtain a functional that captures the many-body effects of embedding an atom in the environment of a solid. The traditional approach is to consider an effective charge density at the position of the ion, which is viewed as a point object, and take a functional of this density to express the energy of embedding. However, the charge density associated with any ion is short-ranged, and the value of the density due to one ion at the position of another ion is essentially negligible. This means that, if realistic densities are to be used, the embedding effect would be minimal and the many-body interactions would have to be represented by the pair potential, which defeats the purpose of having an embedding term.

Instead of the traditional approach, we introduce the following notions. We consider first the contribution of a single ion to the charge density, which can be obtained from equations (3), (4) and (5):

$$Q_i(\boldsymbol{r}) = \left[\sum_{l=0,1} t^{(l)} \left(\rho^{(l)}(r_i)\right)^2\right]^{1/2}, \tag{7}$$

with $r_i = |\boldsymbol{r} - \boldsymbol{R}_i|$ and $\boldsymbol{R}_i$ the position of the ion. For a pair of ions i, j (neglecting the presence of any other ions in the system), we construct the quantity:

$$\rho^{eff}(R_{ij}) = \frac{1}{2}\int \frac{Q_i(\boldsymbol{r})Q_j(\boldsymbol{r})}{Q_i(\boldsymbol{r}) + Q_j(\boldsymbol{r})}\mathrm{d}\boldsymbol{r}. \tag{8}$$

The physical reason for defining this quantity is that the integrand in equation (8) aquires its largest values in the regions *between* ions, precisely where the valence charge is accumulated to form interatomic bonds. The quantity ρ^{eff} is defined so that it has the same dimensions as the Q_i, multiplied by a volume factor, that is, it has the dimensions of charge. Note that once the integral over $\boldsymbol{r}$ is performed in equation (8), ρ^{eff} depends only on the relative distance between ions i and j, $R_{ij} = |\boldsymbol{R}_i - \boldsymbol{R}_j|$. We can now use this quantity to define an effective charge $\overline{\rho}_i$ associated with a particular ion i through equation (2) in the usual manner, which is to be employed in the evaluation of the functional $F(\overline{\rho}_i)$. In this formulation, $\overline{\rho}_i$ now represents the tendency of ion i to form bonds with its neighbours, since the quantities $\rho^{eff}(R_{ij})$ are large when there is significant valence charge to form bonds between ions i and j. In this sense, it is an optimal quantity to use in an embedding functional in order to represent the many-body effects of bonding.

Instead of having to perform the volume integrations, as implied by equation (8), for each pair in a system containing many ions, which would be computationally inefficient, we parametrized the quantity $\rho^{eff}(R_{ij})$ by an expression similar to equation (6), namely

$$\rho^{eff}(R) = \left(A_0 + A_1 R + A_2 R^2\right)^2 \exp(-R/C) \tag{9}$$

and determined the parameters A_0, A_1, A_2, C by fitting again a set of *ab initio* data. In this case, we considered the dependence of the parameters on the lattice constant a_0 (which can also be expressed as a dependence on the volume per atom), choosing the following expressions to represent this dependence:

$$A_n(a_0) = \kappa_n + \lambda_n \exp(-\mu_n a_0), \qquad n = 0, 1, 2 \tag{10}$$

$$C(a_0) = \kappa' + \lambda' a_0 + \mu' a_0^2. \tag{11}$$

To determine the values of these parameters that take into account the dependence on atomic volume, a sufficiently large data base of *ab initio* results must be generated. For the case of Al, we calculated the charge density at 18 different lattice constants in the interval 3.235–4.975 Å, using a sufficiently dense grid to sample the reciprocal space (a $10 \times 10 \times 10$ grid in the Monkhosrt–Pack [19] scheme). The resulting values, used in subsequent calculations, are given in table 2.

With this approach, in essence, we assume changes in the atomic densities due to fluctuations of the interatomic distances R_{ij} at a given lattice constant a_0 to be negligible. We adopted this procedure instead of the dipole charge density that is typically used [5], because it reflects the central idea of the method of embedding an atom in the host density. The resulting $\rho^{eff}(R)$ exhibits physically reasonable behaviour, that is, it has large values in the region of the first neighbourhood ($R = 2.5$–3.2 Å), which has the most important contribution to the embedding function term.

Table 2. Values of the parameters in equations (9) – (11), describing the lattice-constant dependence of $\rho^{eff}(R)$ for Al.

	Value				
Parameter	$n = 0$	$n = 1$	$n = 2$	Parameter	Value
κ_n	1.75236	−2.04912	1.90114	κ'	−0.29589
$\lambda_n \times 10^{-6}$	1.47538	−1.67042	0.35144	λ'	0.22325
μ_n	3.13590	3.10351	2.93016	μ'	−0.02033

Table 3. Values of the parameters that enter in the determination of the energy functional equation (12) and the Morse potential equations (13)–(14).

Parameter	Value	Parameter	Value
b_1	−11.2181495	D(eV)	0.86376
b_2	26.4179007	α(1/Å)	2.1779
b_3	−33.8904348	q	1.2172
b_4	24.4401639	r_0(Å)	2.9703
b_5	−9.1761538	r_c(Å)	6.0268
b_6	1.3857119		

As far as the description of the embedding energy functional is concerned, we used the following expression of the effective density:

$$F(\overline{\rho}_i) = \sum_{n=1}^{6} b_n \left(\overline{\rho}_i\right)^n , \tag{12}$$

where b_n are fitting parameters.

For the pair potential $\phi(r)$, which complements the embedding potential in the total energy expression, equation (1), we adopted a generalized Morse function:

$$\phi(r) = D\left(\exp[-q\alpha(r - r_0)] - q\exp[-\alpha(r - r_0)]\right), \tag{13}$$

where D, q, α, r_0 are the usual Morse potential parameters. In order to ensure that this potential and its first derivatives are continuous and that it is smoothly cut off at $r = r_c$, the following expression is used in computations:

$$\phi_s(r) = \phi(r) - \phi(r_c) + \left(\frac{r_c}{20}\right)\left[1 - \left(\frac{r}{r_c}\right)^{20}\right]\left(\frac{\mathrm{d}\phi}{\mathrm{d}r}\right)_{r=r_c} \tag{14}$$

with the subscript s denoting the smooth version of the potential.

The two components of the functional were fitted together to reproduce the desired properties, including equilibrium lattice constant, bulk modulus and cohesive energy, from experimental measurements, which are actually very close to those of *ab initio* results. In order to ensure that the potential also works well for Al surfaces, we included in the fitting data base the surface energies of three low-index faces as determined by previous calculations [6], since surface energies for individual faces are difficult to obtain from the experiment. We use the unrelaxed atomic configurations for the surface atoms since these are uniquely defined and do not depend on the methodology employed. In table 3 we give the values of $b_n, n = 0, \ldots, 6$, as well as the values of the parameters that enter in the Morse potential, equations (13) and (14), resulting from the fit in the case of Al. These two parts together complete the description of the total energy functional. Figure 3 shows the behaviour of the two components of the functional.

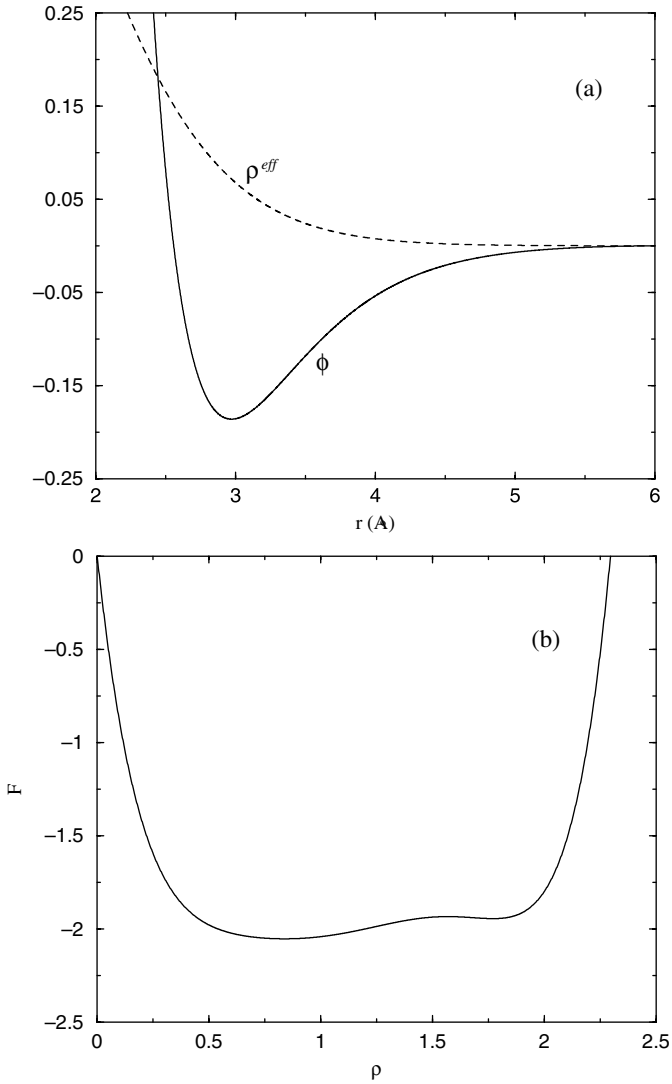

Figure 3. (*a*) The Morse potential $\phi(r)$ (in eV, solid line) and the density $\rho^{eff}(r)$ (- - - -) as functions of the interatomic distance r (in Å). (*b*) The embedding potential $F(\rho)$, as a function of ρ.

3. Application to Al

In order to test the validity of the total energy functional that we obtained above for Al, we performed static calculations at $T = 0$K for the usual bulk properties, such as elastic constants, the vacancy formation energy and the energy and atomic volume of various bulk phases of Al (HCP, BCC, simple cubic-SC) compared with those of the equilibrium FCC phase. As in the case of surfaces, we use again the unrelaxed configuration for the vacancy which is uniquely defined and does not depend on the method employed for the calculation. The results are collected in tables 4 and 5 along with available experimental data and other theoretical values for comparison. The potential reproduces well the most important structural features of Al.

Table 4. Properties of Al as determined by the present work and experiment: a_0 is the lattice constant, E_c is the cohesive energy, B is the bulk modulus, E_V is the vacancy formation energy, C_{ij} are the elastic constants and K is the thermal expansion coefficient. The units and experimental references are given for each physical quantity. Values used in the fitting of the potential are marked by asterisks.

Property	EAM (present work)	Experiment
a_0(Å, 300 K)	4.14	4.05* [24]
E_c(eV/atom)	3.35	3.36* [25]
B(GPa)	85	79* [26]
C_{11}(GPa)	105	114 [26]
C_{12}(GPa)	75	62 [26]
C_{44}(GPa)	49	32 [26]
E_V(eV)	1.20	0.75 [27]
$K(10^{-5}/\mathrm{K})$	1.96	2.4 [24]

Table 5. Surface and bulk properties of Al as determined by the present work and other theoretical studies: γ_s is the surface energy for different low-index surfaces, (110), (100) and (111), in mJ m^{-2}. For the three bulk phases BCC, HCP and simple cubic (SC), ΔV_0 is the difference in atomic volume (in Å^3) and ΔE_c is the difference in cohesive energy (in eV/atom) relative to the corresponding values of the equilibrium FCC phase. Numbers in brackets are from *ab initio* calculations. Values used in the fitting of the potential are marked by asterisks.

	γ_s(110)	γ_s(100)	γ_s(111)
This work	950	870	805
[6]	959*	855*	823*
[7]	1006	943	870
[28]	1100	1020	930
	BCC	HCP	SC
ΔV_0 (Å^3)	0.00 [0.08]	0.00	3.54 [3.26]
ΔE_c (eV/atom)	0.03 [0.08]	0.00	0.41 [0.24]

Beyond the values used in the fit, the elastic constants and the vacancy formation energy are in reasonable agreement with experimental values. Note that since the vacancy formation energy is for the unrelaxed configuration the equilibrium structure including relaxation is expected to produce a better agreement with the experimental value. Moreover, the cohesive energy and atomic volume of the HCP, BCC and SC bulk phases are all higher than the equilibrium FCC phase, although the differences between FCC and HCP are negligible. These results are in reasonable agreement with *ab initio* calculations that we have performed for comparison (the results are shown in table 5).

We also performed microcanonical MD simulations to obtain several thermodynamic quantities. We used a system consisting of 4000 atoms arranged in an FCC lattice, while the equations of motion were integrated by means of the Verlet algorithm and a time step of 5 fs. After the usual equilibration of the system we calculated the thermodynamic averages over trajectrories that lasted 50 ps. From these simulations we obtained the phonon density of states (DOS) at room temperature by Fourier transforming the velocity autocorrelation functions and the temperature dependence of the mean square displacement (MSD) from the atomic density profiles.

In figure 4 we give the calculated phonon DOS at 300 K along with experimental data [20]. The agreement is very satisfactory. By adjusting the lattice constant to get zero pressure at different temperatures in the range from 300 to 900 K, we obtained the

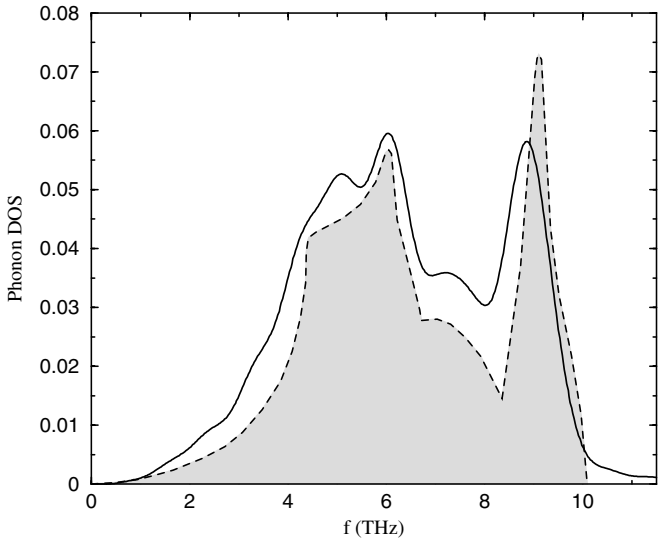

Figure 4. Phonon density of states (DOS) as obtained from the MD simulations at $T = 300$ K (——) and from experiment (- - - -) [20].

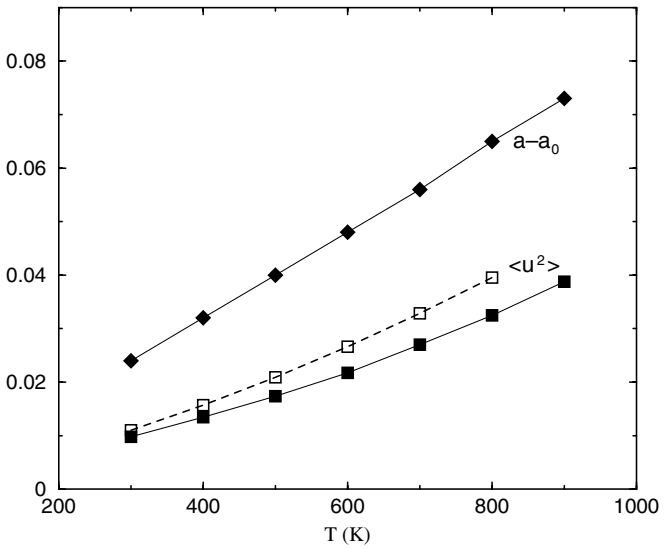

Figure 5. Mean-square displacements $\langle u^2 \rangle$ of bulk Al atoms (squares, in Å^2), and lattice constant relative to its zero-temperature value, $a - a_0$ (rhombuses, in Å), as functions of temperature. Filled symbols correspond to MD results, open symbols correspond to experimental data from [21].

thermal expansion coefficient which is included in table 4 and is in reasonable agreement with the experimental value. The lattice constant deviation from the zero-temperature value $a - a_0$ (where $a_0 = 4.12$ Å) is shown in figure 5. Figure 5 also depicts the temperature dependence of the MSD for the bulk atoms along with the corresponding experimental data [21], determined from x-ray scattering measurements. From the MSD results and using Lindemann's criterion [22] we estimated the thermodynamic melting temperature of the bulk system to be 980 K, in reasonable agreement with the experimental value of 933 K [23].

4. Conclusions

In this work we presented a method for constructing an embedded atom potential model with input from *ab initio* electronic structure calculations. The model is based on charge densities obtained from DFT calculations at different volumes which are used for the determination of an effective electron density, constructed to take into account the contributions of the valence electrons of both the embedded atom and the neighbouring host atoms. We applied the method to Al, for which we performed static calculations and MD simulations for several thermodynamic quantities to compare with available experimental and theoretical results. We find that our approach reproduces satisfactorily the behaviour of the bulk material as well as that of certain important defect properties, like the vacancy formation energy.

In our method the electronic charge density is a realistic quantity, which is reproduced accurately by fitting *ab initio* calculations and is not treated as adjustable parameter in the fitting of the energy functional. In this sense, it should be straightforward to generalize the approach to multicomponent systems, where the density of each element is fit separately and the embedding energy is obtained by simple superposition of the individual densities without changing the embedding functional.

Acknowledgments

This work was supported by the Project HPRN-CT-2000-00038.

References

[1] Norskov J K and Lang N D 1980 *Phys. Rev.* B **21** 2131
[2] Scott M J and Zaremba E 1980 *Phys. Rev.* B **22** 1564
[3] Norskov J K 1982 *Phys. Rev.* B **26** 2875
[4] Daw M S and Baskes M I 1983 *Phys. Rev. Lett.* **50** 1285
[5] Voter A F 1994 *Interemetallic Compounds* vol 1 778 (New York: Wiley)
[6] Voter A F and Chen S P 1987 High Temperature Inter-metallic alloys *Proc. Symposia on Materials Research Society* ed R W Siegel *et al* (MRS, Pittsburgh.) vol 82 p 175
[7] Mishin Y, Farkas D, Mehl M J and Papaconstantopoulos D A 1999 *Phys. Rev.* B **59** 3393
[8] Baskes M I 1992 *Phys. Rev.* B **46** 2727
[9] Foiles S M, Baskes M I and Daw M S 1986 *Phys. Rev.* B **33** 7983
[10] Robertson I J, Heine V and Payne M C 1993 *Phys. Rev. Lett.* **70** 1944
[11] Robertson I J, Thomson D I, Heine V and Payne M C 1994 *J. Phys.: Condens. Matter* **6** 9963
[12] Payne M C, Robertson I J, Thomson D I and Heine V 1996 *Phil. Mag.* B **73** 191
[13] Hohenberg P and Kohn W 1964 *Phys. Rev.* B **136** 864
[14] Kohn W and Sham L J 1965 *Phys. Rev.* **140** A1133
[15] Perdew J P and Zunger A 1981 *Phys. Rev.* B **23** 5048
[16] Modine N A, Zumbach G and Kaxiras E 1997 *Phys. Rev.* B **55** 10289
[17] Waghmare U V, Kim H, Park I J, Modine N, Maragakis P and Kaxiras E 2001 *Comput. Phys. Commun.* **137** 341
[18] Papageorgiou D G, Demetropoulos I N and Lagaris I E 1998 *Comput. Phys. Commun.* **109** 227
[19] Monkshorst H J and Pack J D 1967 *Phys. Rev.* B **13** 5188
[20] Stedman R, Almqvist L and Nilsson G 1967 *Phys. Rev.* **162** 549
[21] Shuka R C and Plint C A 1989 *Phys. Rev.* B **40** 10337
[22] Lindemann F A 1910 *Z. Phys.* **11** 609
[23] Ashcroft N W and Mermin N D 1976 *Solid State Physics* (New York: Holt, Rinehart and Winston)
[24] Kittel C 1986 *Introduction to Solid State Physics* (New York: Wiley-Interscience)
[25] Weast R C (ed) 1984 *Handbook of Chemistry and Physics* (Boca Raton, FL: CRC Press)
[26] Simons G and Wang H 1977 *Single Crystal Elastic Constants and Calculated Aggregate Properties* (Cambridge MA: MIT Press)
[27] Koehler J S 1970 *Vacancies and Interstitials in Metals* ed A Seeger *et al* (Amsterdam: North-Holland)
[28] Sinnot S B, Stave M S, Raeker T J and DePristo A 1991 *Phys. Rev.* B **44** 8927